

Simulation and Experimental Studies of Phase Shift and Adhesion in Biological Tissues

Naoki Tano^{1†}, Ren Koda², Yoshiki Yamakoshi^{1,2}, and Marie Tabaru^{1*} (¹IIR, Tokyo Tech; ²Gunma Univ.)

1. Introduction

Froze shoulder, a condition that limits the range of motion (ROM) in shoulder, has a high prevalence rate of 76% among diabetic patients¹. One of the causes is considered to be the adhesion between the soft tissues surrounding the joint². A dynamic ultrasonography study has been conducted to investigate these adhesions. Fujiwara et al. introduced a method to quantitatively assess the adhesion state using the stretching velocity ratio between the deltoid muscle and the subscapularis³.

Meanwhile, continuous shear wave elastography (C-SWE) employs an external mechanical vibrator to excite shear waves inside the human body^{4,5}. The vibrator in C-SWE can induce micro displacements in tissue, making it a quasi-dynamic measurement without requiring patient movement⁶. This study focused on observing the propagation of shear waves continuously excited in C-SWE, investigating the influence of tissue adhesion on their phase. Here, the effects of adhesion were experimentally examined through simulations and phantom studies designed to replicate tissue adhesion.

2. 2D-FDTD Simulation of Tissue Adhesion

The effect of tissue adhesion on shear wave propagation is simulated by 2D-FDTD (finite-difference time-domain) method. The FDTD simulation is derived from the equation of motion and strain-velocity relationship, presented as followed.

$$\frac{\partial v_x}{\partial t} = \frac{1}{\rho} \frac{\partial \sigma}{\partial z}, \quad (1)$$

$$\frac{\partial v_z}{\partial t} = \frac{1}{\rho} \frac{\partial \sigma}{\partial x}, \quad (2)$$

$$\frac{\partial \sigma}{\partial t} = \mu \left(\frac{\partial v_z}{\partial x} + \frac{\partial v_x}{\partial z} \right) + \eta \left(\frac{\partial v_z}{\partial x} + \frac{\partial v_x}{\partial z} \right), \quad (3)$$

where v_x , v_z , and σ stand for particle velocities along the x and z axes, and shear stress. Additionally, ρ , μ , and η are the physical property values of the medium, specifically density, shear elastic modulus, and viscosity coefficient.

The adhesion strength affects the strength of the impact of velocity and shear stress from neighboring particles at the adhesion interface.

Therefore, we introduced the adhesion coefficient k into the basic equations of Equation (1) to (3), as follows:

$$\frac{\partial v_x}{\partial t} = \frac{k_z}{\rho} \frac{\partial \sigma}{\partial z}, \quad (4)$$

$$\frac{\partial v_z}{\partial t} = \frac{k_x}{\rho} \frac{\partial \sigma}{\partial x}, \quad (5)$$

$$\frac{\partial \sigma}{\partial t} = \mu \left(k_x \frac{\partial v_z}{\partial x} + k_z \frac{\partial v_x}{\partial z} \right) + \eta \left(k_x \frac{\partial v_z}{\partial x} + k_z \frac{\partial v_x}{\partial z} \right), \quad (6)$$

where k_x and k_z are adhesion coefficients in the corresponding axes. Since these coefficients determine the influence from the neighboring particles, higher coefficient values within the range of 0 to 1.0 indicates the stronger adhesion conditions.

Fig. 1-a shows the shear wave phase map at different adhesion coefficients. The phase map at $k_z = 1.0$ shows no phase changes in the propagated shear wave as it can be regarded as a continuous continuum without adhesion interfaces. In contrast, the less adhesive model at $k_z = 0.1$ causes a shift in the shear wave phase at the adhesion interface. However, it should be noted that in this simulation model, k_x was consistently set to 1.0, while k_z was assigned a specific value only at $z = 10$ and 11 mm. The plots in Fig. 1-b represent the relationship between

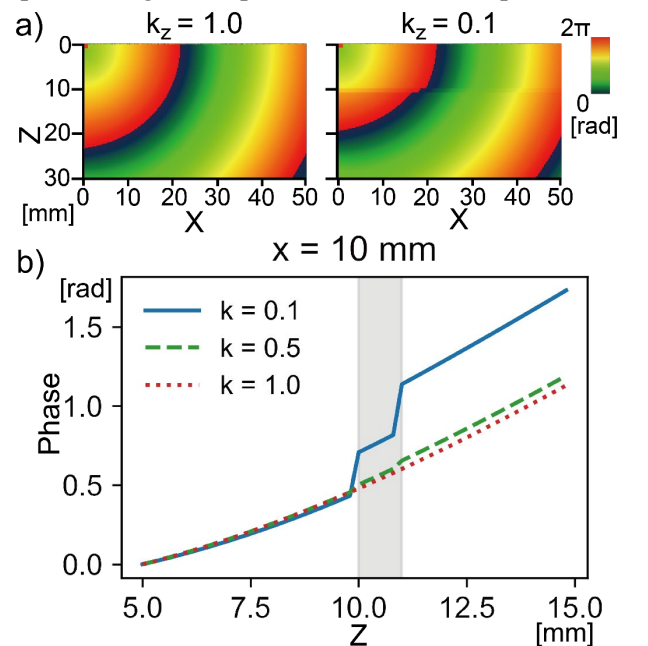


Fig. 1 Simulated shear wave propagation. a) Phase maps at $k_z = 1.0, 0.1$. b) Phase plot around adhesion interface.

E-mail: [†]tano.n.aa@m.titech.ac.jp,

^{*}tabaru.m.ab@m.titech.ac.jp

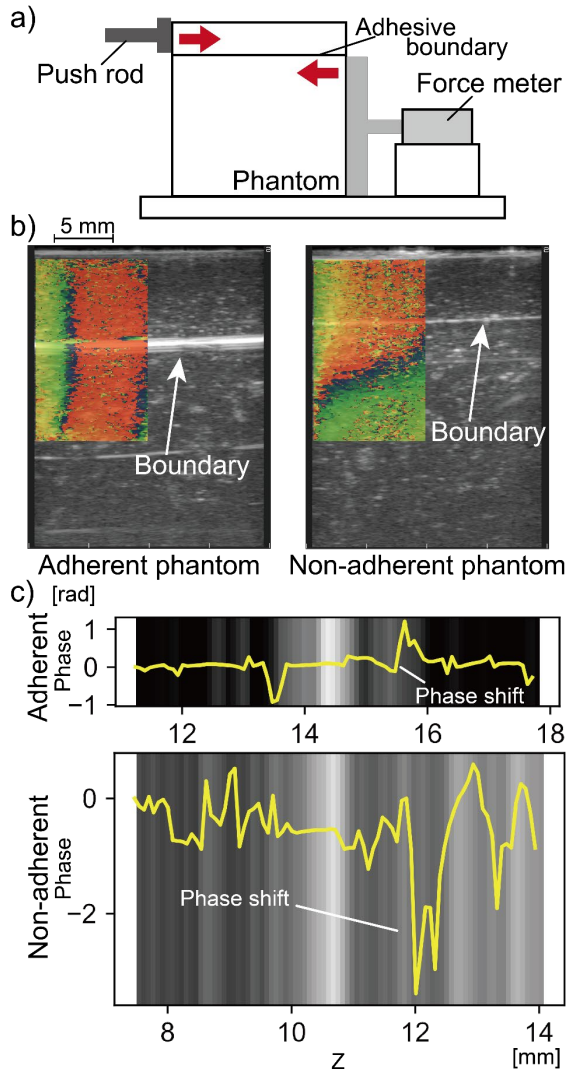


Fig. 2: Measurement of adhesion strength and shear wave propagation in the phantom. a) A diagram of a compression shear adhesion strength test. b) Phase maps of an adherent phantom (left) and a non-adherent phantom (right). c) Phase plot at $x = 20$ mm in an adherent and a non-adherent phantom. Background color corresponds to the B-mode values.

the adhesion coefficient and the amount of phase shift around the adhesive interface. The plot indicates that the phase shift of shear waves between the two layers across the adhesion interface becomes larger as the adhesion condition weakens.

3. Phantom Experiments

Phantoms with different adhesive levels were fabricated to observe shear wave propagation under varying adhesion conditions. The phantom tissue was created by dissolving agar powder (Basic Grade Agar Powder; Nichie) in water at a concentration of 1% and then solidifying it. To simulate adhesion, the phantom was divided into two layers, with the second layer was poured when the first layer cooled to 50°C . The non-adherent

condition was achieved by placing a thin plate between the two layers, which was removed after the layers solidified. Adhesive strength was evaluated by a compression shear adhesion strength test, as illustrated in Fig.2-a. The measured adhesion strengths for the adherent and non-adherent phantom were 809 Pa and 226 Pa, respectively.

Fig. 2-b demonstrates the shear wave propagation in the phantom tissues. A difference in the propagation angle of the shear wave between the first and second layers was noted. This resembles the propagation pattern observed around $x = 30$ mm in Fig.1-a. Furthermore, the amount of phase shift also increased in non-adherent phantom as shown in Fig. 2-c. The phase shift after adhesion interface was 1.3 rad and 3.4 rad in adherent and non-adherent phantom, respectively.

4. Discussion & Conclusion

This work experimentally observed the influence of tissue adhesion on shear wave propagation through simulation and phantom study. A change in propagation pattern was seen at the adhesion interface. Meanwhile, future work aims to perform in-vivo measurements and extract a quantitative index for the evaluation of adhesion.

Acknowledgment

This work was supported by JSPS KAKENHI Grant Number JP22K04134, the Cooperative Research Project of Research Center for Biomedical Engineering, JKA, and JKA's promotion funds from KEIRIN RACE.

References

- 1) Juel N. G., Brox J. I., Brunborg C., Holte K. B., Berg T. J., *Arch Phys Med Rehabil*, 98, 1551–1559 (2017).
- 2) Ha'eri G. B., Maitland A., *J Rheumatol*, 8, 149–152 (1981).
- 3) Fujiwara M., Hermawan N., Suenaga T., Hagiwara Y., Saijo Y., *JSES Int*, (2024).
- 4) Yamakoshi Y., Sato J., Sato T., *IEEE Trans Ultrason Ferroelectr Freq Control*, 37, 45–53 (1990).
- 5) Koda R., Kuwabara T., Tano N., Tabaru M., Tanigawa S., Kamiyama N., Yamakoshi Y., *Jpn J Appl Phys*, 63, 04SP82 (2024).
- 6) Tabaru M., Koda R., Shitara H., Chikuda H., Yamakoshi Y., *Journal of Medical Ultrasonics*, 1–12 (2024).
- 7) Tano N., Koda R., Tanigawa S., Kamiyama N., Yamakoshi Y., Tabaru M., *Ultrason Imaging*, 46, 197–206 (2024).